Published in final edited form as:
J Neurosci. 2001 July 1; 21(13): 4864–4874.

Contrasting Effects of Ibotenate Lesions of the Paraventricular Nucleus and Subparaventricular Zone on Sleep–Wake Cycle and Temperature Regulation

J. Lu[1], **Y.-H. Zhang**[1], **T. C. Chou**[1], **S. E. Gaus**[1], **J. K. Elmquist**[1], **P. Shiromani**[2], and **C. B. Saper**[1]

[1]Department of Neurology and Program in Neuroscience, Beth Israel Deaconess Medical Center, Harvard Medical School, Boston, Massachusetts 02115

[2]Department of Psychiatry, Brockton Veterans Administration Hospital, Harvard Medical School, Boston, Massachusetts 02115

Abstract

The suprachiasmatic nucleus (SCN), the circadian pacemaker for the brain, provides a massive projection to the subparaventricular zone (SPZ), but the role of the SPZ in circadian processes has received little attention. We examined the effects on circadian rhythms of sleep, body temperature, and activity in rats of restricted ibotenic acid lesions of the ventral or dorsal SPZ that spared the immediately adjacent paraventricular hypothalamic nucleus (PVH) and the SCN. Ventral SPZ lesions caused profound reduction of measures of circadian index of sleep (by 90%) and locomotor activity (75% reduction) but had less effect on body temperature (50% reduction); dorsal SPZ lesions caused greater reduction of circadian index of body temperature (by 70%) but had less effect on circadian index of locomotor activity (45% reduction) or sleep (<5% reduction). The loss of circadian regulation of body temperature or sleep was replaced by a strong ultradian rhythm (period ~3 hr). Lesions of the PVH, immediately dorsal to the SPZ, had no significant effect on any circadian rhythms that we measured, nor did the lesions affect the baseline body temperature. However, the fever response after intravenous injection of lipopolysaccharide (5 μg/kg) was markedly decreased in the rats with PVH lesions (66.6%) but not dorsal SPZ lesions. These results indicate that circadian rhythms of sleep and body temperatures are regulated by separate neuronal populations in the SPZ, and different aspects of thermoregulation (circadian rhythm and fever response) are controlled by distinct anatomical substrates.

Keywords

circadian rhythm; ultradian rhythm; ibotenic acid; suprachiasmatic nucleus; c-Fos; fever

The suprachiasmatic nucleus (SCN) of the hypothalamus controls the circadian rhythms of behavioral and physiological states, including sleep–wake cycles and body temperature in mammals (Ibulka and Kawamura, 1975; Mouret et al., 1978; Eastman et al., 1984; for review, see Harrington et al., 1994). Although remarkable progress has been made in revealing molecular mechanisms of circadian rhythm within the mammalian SCN in the last few years (for review, see Dunlap, 1998), the output pathways by which the SCN exerts control over circadian rhythms are not well understood.

Correspondence should be addressed to Dr. C. B. Saper, Department of Neurology, Beth Israel Deaconess Medical Center, 330 Brookline Avenue, Boston, MA 02215. csaper@caregroup.harvard.edu.

By far the densest SCN projections are to the subparaventricular zone (SPZ) (Watts and Swanson, 1987; Watts et al., 1987; Watts, 1991). The SPZ is defined by the SCN terminal field, beginning at the dorsal border of the SCN [the ventral SPZ (vSPZ)] and continuing dorsally and caudally into the region ventral to the paraventricular nucleus [the dorsal SPZ (dSPZ)]. Many SCN fibers extend farther caudally into the medial part of the dorsomedial hypothalamic nucleus (DMH). Because of its relationship with the SCN, this output pathway has been proposed as a major component of the outflow for circadian regulation (Watts, 1991). This hypothesis is supported by the observation that electrolytic lesions including the DMH and the dorsal SPZ abolish circadian rhythms of feeding, drinking, and corticosterone secretion (Bernardis, 1973; Bellinger et al., 1976; Cipolla-Neto et al., 1988). These studies do not distinguish between the effects of injuring cell bodies versus fibers of passage, but suggest that the SPZ plays an important role in circadian regulation.

The parvicellular divisions of the paraventricular nucleus of the hypothalamus (PVH) also receive a small part of the output of the SCN (Vrang et al., 1995a). Dorsal parvicellular PVH neurons project to the sympathetic preganglionic column in the spinal cord (for review, see Saper, 1995), where they regulate the nocturnal secretion of melatonin (Klein et al., 1983). Medial parvicellular neurons in the PVH secrete corticotropin-releasing hormone into the median eminence, thereby regulating the diurnal secretion of adrenal corticosteroids. It is not known, however, whether the circadian control of these functions is exerted by direct SCN inputs to the PVH or by relays through the SPZ, for example to the caudal DMH, which supplies a major projection back to the PVH (Elmquist et al., 1998). In addition, it is not known to what extent the cycles of melatonin and adrenal corticosteroid secretion mediated by the PVH influence other circadian functions, such as sleep or body temperature.

To determine and differentiate the roles of the SPZ and the PVH in the circadian regulation of sleep, activity, and body temperature cycles, we have placed small ibotenic acid lesions in the SPZ (ventral and dorsal subdivisions) and PVH and examined circadian rhythms of sleep, activity, and body temperature. We also tested the effects of these lesions on fever response after intravenous injection of lipopolysaccharide (LPS).

MATERIALS AND METHODS

Animals

Pathogen-free adult male Sprague Dawley rats (275–300 gm; $n = 69$) purchased from Taconic (Germantown, NY) were used. The rats were individually housed and had *ad libitum* access to food and water. All animals were housed under controlled conditions (12 hr light starting at 7:00 A.M.; 200 lux) in an isolated ventilated chamber maintained at 20–22°C. All protocols were approved by the Institutional Animal Care and Use Committees of Beth Israel Deaconess Medical Center and Harvard Medical School.

Venous catheterization and thermal telemetry transmitter

All surgeries were performed under chloral hydrate anesthesia (7% in saline, 0.35 gm/kg) using aseptic techniques. During the preliminary surgical session, a temperature/activity transmitter (type TA10-F40, Data Science International) was implanted in each animal via a ventral midline incision into the peritoneal cavity. In some animals who needed venous access for later injections of LPS, a 2 cm incision was made along the medial thigh, and the femoral vein was exposed. A SILASTIC catheter containing heparinized saline (10 U/ml of saline) was inserted into the vein and sutured in place. The free end of the catheter was passed under the skin, exteriorized between the scapulas, and plugged with a sterile wire stylet. All wounds were closed with wound clips, and animals were allowed to recover for 3

d, after which body temperature and activity data were recorded every 5 min to provide a prelesion baseline.

Ibotenic acid injection and EEG/EMG implantation

It was necessary to have a second surgical session to place a lesion in the SPZ or PVH. The scalp was incised, and a burr hole was made at the injection site. A fine glass pipette containing ibotenic acid was lowered into the SPZ or PVH stereotaxically. The coordinates used for the PVH (Paxinos and Watson, 1986) were anteroposterior (AP) −1.8 mm, dorsoventral (DV) −7.2 mm, mediolateral (ML) ±0.5 mm relative to bregma. For the dorsal SPZ, we used AP −1.8 mm, DV −7.6 mm, ML −0.5 mm; for ventral SPZ, we used AP −1.3 mm, DV 8.0 mm, ML ±0.4 mm. The tooth bar was 3.3 mm below the ear bar. Twenty nanoliters containing 10 nmol ibotenic acid (Sigma, St. Louis, MO) in saline was injected by air pressure through a glass pipette. After 2 min, the pipette was slowly withdrawn.

EEG/EMG electrodes could be implanted only after the ibotenic acid lesions were made, because the implantation procedure obscured skull landmarks necessary for accurate placement of ibotenic acid injections. Four screw electrodes were implanted into the skull, in the frontal (two screws) and parietal bones (two screws) of each side, and two flexible wire electrodes were placed in the nuchal muscles. The electrodes were soldered in sockets that were connected via flexible recording cables and a commutator to a Grass polygraph and computer.

Analyses of physiological data

The EEG/EMG signals were amplified by a polygraph (Grass) and digitized by an Apple Macintosh computer running ICELUS (G Systems, Inc). Wake–sleep states were manually scored in 12 sec epochs of the digitized EEG/EMG. Wakefulness was identified by the presence of desynchronized EEG and phasic EMG activity. Non-rapid eye movement (NREM) sleep consisted of high amplitude slow wave EEG together with low EMG tone relative to waking. REM sleep was identified by the presence of regular theta EEG activity coupled with low EMG tone relative to NREM sleep. The amount of time spent in wake, NREM sleep, and REM sleep was determined for each hour. Body temperature and activity were monitored with Minimitter telemetry antennas placed under the cages of individual animals. Activity recordings with this apparatus reflect movement of the implanted transmitter with respect to the antenna. Signals were averaged over 5 min and recorded on a Macintosh computer running Minimitter software.

Perfusion and immunohistochemistry

The rats were deeply anesthetized with chloral hydrate (350 mg/kg, i.p) and perfused with saline (100 ml) and then 10% neutral buffered formalin (500 ml) transcardially. The brains were cut coronally at 40 μm in four series. The sections were washed in PBS and incubated with primary antiserum in PBS containing 0.25% Triton X-100 [c-Fos, Ab-5, 1:150,000 (Oncogene); arginine vasopressin (AVP) 1:10,000 (Peninsula Laboratories, Belmont, CA); vasoactive intestinal polypeptide (VIP) 1:100,000 (Chemicon, Temecula, CA)] for 1 d at room temperature. The sections were washed again in PBS and incubated in biotinylated secondary antiserum (1:1000; Jackson ImmunoResearch, West Grove, PA) for 1 hr, washed, and incubated in ABC regents (1:1000; Vector Laboratories, Burlingame, CA) for 1 hr, then washed again and incubated in a 0.06% solution of 3,3-diaminobenzidine tetrahydrochloride (DAB; Sigma) and 0.05% CoCl and 0.01% $NiSO_4$ (NH4) in PBS plus 0.02% H_20_2 for ~5 min. Finally, the sections were mounted on slides, dehydrated, cleared, and coverslipped.

Nissl staining

A series of adjacent sections was mounted on gelatin-coated slides, washed, and incubated in 0.25% thionin solution for 2 min, then washed and dehydrated in gradient ethanols, and cleared in xylene before being coverslipped.

Determination of lesion region

The area of the lesion was determined by loss of neurons and presence of gliosis in Nissl-stained sections. To further verify the lesion in specific areas, we combined the immunostaining for c-Fos, VIP, and AVP. In the SCN, the ventrolateral division contains VIP-immunoreactive (ir) neurons, whereas the dorsomedial division contains AVP-ir neurons. In the PVH, AVP-ir neurons are found mainly in the magnocellular subdivision. By using immunostaining for these peptides, we could determine whether the lesions included the SCN or the PVH and whether the lesions affected the fibers of passage through the SPZ. Because LPS induces Fos expression in the PVH, we also used loss of Fos-ir neurons in the PVH to assess the integrity of the PVH after LPS administration. Because most of the cells in the SPZ do not contain any single known neurotransmitters, we used VIP-ir axons (see Fig. 1) to delineate the SPZ and used counting of Nissl-stained cells within the VIP axonal field of the SPZ to determine loss of cells.

Cell counting in the SPZ and PVH

For the dorsal SPZ, we diagonally placed a box (300 × 200 μm) along the ventral border of the PVH at a level corresponding to 1.7 mm posterior to bregma in the atlas of Paxinos and Watson (1986). For the ventral SPZ, we counted cells in a vertical box (100 × 300 μm) 100 μm lateral to the third ventricle, with the bottom edge directly above the dorsal border of the SCN, at a level corresponding to 1.5 mm posterior to bregma in the atlas of Paxinos and Watson (1986). For the PVH, we placed a box (500 × 300 μm) horizontally, 100 μm lateral to the third ventricle with its upper border at the same level as the most dorsal point of the third ventricle at the level equivalent to 1.8 mm posterior to bregma in the atlas of Paxinos and Watson (1986).

Animals with bilateral cell loss >70% in the counting areas were considered to have substantial lesions, and animals with no lesion (for example, injections into the third ventricle) were used as the controls. We used the entire series of animals to determine whether the degree of cell loss in the specific target area correlated with the physiological response.

Data analyses of circadian rhythm: circadian index and cosinor amplitude

The circadian index (CI) for a physiological variable was calculated as $CI = (mean_{night} - mean_{day})/mean_{24hr}$, scaled to an index of 100 for the mean for the control animals. For sleep, the mean percentage of the 12 hr period (night and day) spent in total sleep was calculated and used to determine the circadian index. For body temperature, the mean of temperature recorded every 10 min across the 12 hr period was used. Total activity was summated over the entire 12 hr period. The “night” cycle corresponded to the 7:00 P.M.–7:00 A.M. period, and “day” corresponded to 7:00 A.M.–7:00 P.M., even when the animals were kept in a completely dark environment. Animals kept in a dark environment for 6 d showed minimal drift in their circadian phase. Using cosinor analysis, there was a phase delay of 23.7 ± 14.6 min for body temperature peak in the control animals on day 6 in constant darkness (DD), and 20.4 ± 16.8 min for the animals with vSPZ lesions. Animals with dSPZ lesions had a phase delay in sleep peak by 34.3 ± 20.7 min. Because the phase delays were so small, and because they had to be measured on different variables (because of differential reduction of

sleep vs body temperature circadian amplitude with different lesions), we did not correct for the circadian phase in determining circadian index.

As a further control for the circadian index as a measure of circadian amplitude, we therefore also used cosinor analysis to determine the amplitudes of circadian rhythms of sleep, body temperature, and activity, independent of circadian phase, for the last 48 hr of the continuously dark period. Briefly, the cosinor amplitude (A) was determined by:

$$A = \sqrt{C^2 + S^2},$$

when:

$$C = \sum_{n=0}^{47} X_n \cos\left(\frac{2\pi n}{24}\right), \quad S = \sum_{n=0}^{47} X_n \sin\left(\frac{2\pi n}{24}\right),$$

and then was scaled so that the mean for the control animals was 100. We found that the amplitude derived from cosinor analysis was consistent with the circadian index (see Results).

In addition to the circadian index and cosinor analysis, we also used a *t* test to determine whether there was a significant difference between the means of physiological variables during the day and the night. Values are expressed throughout this text as mean ± SEM.

Experimental protocol

The effects of lesions in the SPZ and PVH on circadian rhythmicity—During the prelesion control period, we continuously recorded body temperature and activity for 3 d. Beginning 1 d after the ibotenic acid lesions were placed, we recorded EEG/EMG, body temperature, and activity continuously in both lesion and control animals for the next 6 d under a 12 hr light/dark schedule (LD) and then for 6 more days under DD. Data for the cosinor analysis of amplitude of circadian rhythms of sleep, body temperature, and locomotor activity were collected during the last 48 hr of the DD period; the circadian index was measured on data from the last 24 hr of the DD period.

We used two groups of control animals (controls for vSPZ lesion = 7; controls for dSPZ lesion = 10) because the experiments were performed in two series a few months apart. The control animals in each series were animals drawn from the series in which the injections of ibotenic acid had been made into the third ventricle, and no lesions in the hypothalamus were found. Rats that had >70% loss of cells in the vSPZ (n = 8), dSPZ (n = 7), or PVH (n = 7) bilaterally were identified as having substantial lesions. The animals with 20–70% cell loss bilaterally in the vSPZ (n = 10) or dSPZ (n = 10) were compared with them by correlation analyses to assess whether the observed physiological effects correlated with cell loss in the SPZ. This is an important component of the analysis, because the lesions always extend beyond the intended target, including variable amounts of adjacent tissue. We found in our earlier work that some effects seen in animals with substantial lesions (e.g., in the ventrolateral preoptic nucleus) were not correlated with cell loss in that structure, thus allowing us to determine that the effects arose from adjacent structures (Lu et al., 2000).

The effects of lesions in the PVH and SPZ on fever response—To examine fever responses in animals with either PVH (n = 7) or dSPZ lesions (n = 7), dSPZ controls (n = 10) were returned after recording in a DD cycle for 6 d to a 12 hr LD schedule (light on 7:00

A.M.). After a further 3 d for adaptation, during which they were handled daily, the animals received an intravenous injection of 5 μg/kg LPS (*Salmonella typhimurium*, Sigma) at 10:00 A.M. and then were perfused at 3 P.M. The 5 hr (10:00 A.M. – 3 P.M.) delay after LPS injections allowed us to measure dynamic changes in body temperature and then to determine expression of Fos protein in the brains by immunohistochemistry (Elmquist et al., 1996).

RESULTS

Defining lesions of the SPZ and PVH

Although Watts and colleagues (1987) originally described the SPZ based on the tendency for SCN axons to terminate ventral to the PVH rather than within it, the name SPZ does not fully describe the region. As defined by the continuous column occupied by dense SCN axonal arborization and termination, the SPZ begins just dorsal to the SCN (Fig. 1*A, B*) where it overlaps with the peri-SCN region. As the SCN axons progress caudally, the terminal zone becomes progressively more dorsal to occupy the region just ventral to the PVH (Fig. 1*C*). It is possible in Nissl-stained sections to identify the SPZ by the presence of bundles of dorsoventrally oriented axons piercing the medial part of the anterior hypothalamic area. At the level of the PVH, the SCN termination zone turns laterally, running just ventral to the PVH. However, relatively few SCN axons further penetrate the PVH capsule; instead, the remaining SCN axons continue caudally to terminate diffusely throughout the rostromedial DMH. Even more caudally, a few axons terminate in the caudal DMH (Fig. 1 *D*) but avoid its compact subnucleus. We defined the vSPZ as the region of SCN terminals in the medial part of the anterior hypothalamic area for ~1 mm dorsal and caudal to the SCN and the dSPZ as the more caudal part of the SPZ centered on the area ventral to the PVH. The SCN terminal field continues back into the DMH, which is continuous with the SPZ, and receives substantial SPZ inputs (Elmquist et al., 1998).

We defined the cell loss in our animals by using a combination of Nissl, c-Fos, AVP, and VIP staining. The extent of vSPZ lesions was defined by Nissl cell counts within the region identified by VIP fibers at the level of the SCN, and the extent of dSPZ lesions was defined by counts at the level of the PVH (see Materials and Methods). To determine whether the SCN was injured in our vSPZ lesions, we used immunostaining for AVP, VIP, and Fos staining in addition to Nissl staining. In most cases, we found that there was no morphological damage to neurons in the SCN, which generally appeared resistant to ibotenic acid (Fig. 2*A–C*); if the SCN was damaged, the case was excluded from the analysis. Dorsal SPZ lesions in general did not injure the PVH as judged by loss of Nissl- or AVP-stained neurons within the nucleus, or by loss of Fos-ir neurons after LPS stimulation (Fig. 2*D–F*). The PVH lesions usually included a small but variable number of cells in the dSPZ as determined by counts of Nissl-stained neurons in the region marked by VIP fibers (Fig. 2*G–I*). The locations of lesions in selected animals of all three groups are illustrated in Figure 3.

The effects of SPZ lesions on circadian rhythms of body temperature, sleep, and activity

Ventral SPZ—We obtained 8 rats with >70% cell loss bilaterally in the vSPZ and 10 rats that had cell loss ranging from 20 to 70%. None of our lesions appeared to affect neuronal morphology in the SCN as judged by AVP, VIP, Nissl, and Fos staining (Fig. 2 *A–C*). We did not analyze animals in which the vSPZ was damaged only unilaterally. For controls, we used animals (n = 7) that had injections into the third ventricle without apparent damage to the SCN or the SPZ.

Typical lesions in this group included the vSPZ and often infringed on the rostroventral edge of the dSPZ (Fig. 3). VIP and AVP fibers in the vSPZ were intact (Fig. 2*B, C*). In the

animals with vSPZ lesions, sleep, body temperature, and activity were synchronized to day/night cycles while on an LD 12 hr cycle (Fig. 4*A*). In constant darkness, the animals with vSPZ lesions lost their circadian rhythms of sleep (CI = 9.8 ± 4.7, mean ± SEM; compared with controls, $p < 0.01$; cosinor amplitude = 14.8 ± 4.1, compared with controls, $p < 0.01$) (Figs. 5, 6). Daytime total sleep averaged 56.8 ± 2.9%, which was not significantly different from night sleep time, at 50.1 ± 3.3%, $p > 0.05$. These animals also lost circadian rhythm of activity [CI = 27.0 ± 6.2, $p < 0.05$; cosinor amplitude 22.1 ± 3.7, $p < 0.01$ (Fig. 7); daytime activity 2.2 ± 0.3 U, night-time activity 2.8 ± 0.4, $p > 0.05$ (Fig. 5)]. Body temperature retained a statistically significant circadian rhythm as determined by comparison of body temperature during the day (37.3 ± 0.04°C) and night (37.7 ± 0.05°C; $p < 0.05$) (Fig. 4*A*), but the amplitude of the rhythm was about half as great as in controls (CI = 48.7 ± 11.5; cosinor amplitude = 68.1 ± 4.2; both different from controls at $p < 0.05$) (Fig. 7). A strong ultradian component of sleep and body temperature emerged after vSPZ lesions, with a period of ~3–3.4 hr corresponding to seven to eight cycles across 24 hr. This ultradian rhythm was superimposed on the remaining underlying circadian rhythm of body temperature (Fig. 5*B*). Sleep tended to occur during the troughs between body temperature circadian peaks, whereas locomotor activity corresponded to the body temperature peaks. Alternating ultradian peaks of sleep and locomotor activity were also noted during the night (waking) cycle and may have been associated with minor variations in body temperature (Fig. 5*A*).

Furthermore, across the entire group of animals with 20–70% loss of neurons bilaterally in the SPZ, we found that the number of Nissl-stained neurons in the vSPZ was significantly correlated with the circadian indices of sleep ($r = 0.80$; $p < 0.01$) and activity ($r = 0.63$; $p < 0.05$) but not that of body temperature ($r = 0.51$; $p > 0.05$) (Fig. 8).

Dorsal SPZ—We obtained 7 rats that had >70% cell loss bilaterally in the dSPZ (Fig. 2*D–F*) and 10 rats that had cell loss ranging from 20 to 70% that were used for correlation analysis. In these rats, we avoided damaging the vSPZ region by placing the lesion center more dorsally and caudally. As a result, dSPZ lesions usually included the rostral edge of the DMH. We did not use any animal with a unilateral dSPZ lesion for correlation analysis. Ten rats that had injections in the third ventricle were used as controls.

Immediately after bilateral lesions in the dSPZ, body temperature showed greatly reduced circadian rhythmicity even under light/dark conditions (CI = 30.1 ± 5.3 on days 1–3; cosinor = 40.5 ± 3.9; $p < 0.05$) (Fig. 4*B*). Instead, a robust ultradian rhythm (with a period of ~3 hr, similar to that found after vSPZ lesions) clearly emerged, and its amplitude reached as high as 1.0°C (Figs. 4*B*, 9*A*). By 6 –7 d after the lesion, body temperature began to synchronize to the light/dark cycle with a low circadian amplitude (daytime body temperature 37.6 ± 0.05°C, nighttime 37.3 ± 0.04°C; $p < 0.01$). When the same rats were placed in constant darkness, the circadian temperature rhythm was reduced further (daytime 37.5 ± 0.04°C; nighttime 37.3 ± 0.04°C) (Fig. 4*B*) to the point where there was no statistically significant difference between phases ($p > 0.05$), and there was a reduction of CI to 32.5 ± 7.4 and cosinor amplitude to 44.6 ± 4.2 (both different from controls at $p < 0.05$) (Fig. 7). The same lesions had no significant effects on circadian rhythms of sleep in either the light/dark cycle or constant darkness [in constant darkness, CI = 96.6 ± 4.9; cosinor amplitude = 95.6 ± 2.8, not different from control at $p > 0.05$ (Fig. 7); daytime sleep 63.8 ± 5.8% of total time, nighttime 43.5 ± 5.4%, day and night significantly different at $p < 0.05$ (Figs. 9, 10)]. When we plotted delta power (0.5– 4 Hz) and body temperature in the animals with the dSPZ lesions on the same axes, we found that although the circadian rhythm of body temperature was abolished, sleep episodes still usually occurred at the trough of ultradian body temperature variations, whereas bouts of locomotor activity tended to occur during the ultradian body temperature peaks (Fig. 9*A*).

Although the circadian rhythm of locomotor activity was decreased in the animals with dSPZ lesions (CI = 55.5 ± 16.5; cosinor amplitude = 69.4 ± 11.9), it was not statistically significantly different from the controls ($p > 0.05$) (Fig. 7).

The correlation analysis showed a significant linear correlation of the number of surviving neurons in the dSPZ with the CI of body temperature ($r = 0.71$; $p < 0.05$) but not sleep ($r = 0.24$; $p > 0.05$) or activity ($r = 0.58$; $p > 0.05$) (Fig. 11). Taken together, dSPZ lesions significantly reduced circadian rhythms of body temperature by ~60–70% but had much smaller effects on locomotor activity that were not statistically significant. Sleep showed nearly normal circadian patterning, but a strong ultradian pattern of both body temperature and sleep emerged.

The effects of lesions of the PVH on circadian rhythms

We obtained 7 rats that had substantial bilateral (>70%) lesions of the PVH and 10 rats with <50% cell loss in the PVH or with both injections into the third ventricle that were used as controls. Lesions typically destroyed most cells in the dorsal and medial parvicellular PVH that show Fos expression during fever (Figs. 2*G,I*), but some cells in the periventricular PVH were often spared. The lesions were verified by Fos, Nissl, and AVP staining (Figs. 2*G–I*).

Bilateral PVH lesions did not affect the circadian rhythms of body temperature, sleep, or activity in the light/dark condition or in constant darkness (Figs. 4*B*, 7, 9, 10). The circadian index of body temperature, sleep, and locomotor activity was not different from that of the controls (CI of body temperature = 102.5 ± 33.3; sleep = 98.3 ± 8.6; activity = 98.6 ± 21.3; $p > 0.05$ for all three) (Fig. 7). In parallel, the cosinor amplitudes of sleep, body temperature, and activity showed no difference from the controls (sleep = 86.3 ± 3.2, body temperature = 106.3 ± 8.5, activity = 88.5 ± 12.5) (Fig. 7).

The effects of lesions of the dorsal SPZ and the PVH on fever responses

After administration of LPS to the animals with dSPZ lesions, the fever response was identical to control animals, rising 1.1 ± 0.2°C in animals with dSPZ lesions 5 hr after LPS injection, compared with 1.2 ± 0.2°C in control animals ($p > 0.05$) (Fig. 12). The expression of Fos protein in the PVH, the ventromedial preoptic nucleus (VMPO), and the nucleus of solitary tract (NTS) was likewise identical in the two groups (Table 1).

In the rats with PVH lesions, after intravenous LPS injection, fever was reduced by 66.6% (Fig. 12), and few Fos-ir cells were found in the PVH (Table 1; Fig. 2*H*), although Fos expression in the VMPO and NTS was identical to that of normal controls.

DISCUSSION

The principal findings of this study were that lesions of the vSPZ profoundly disrupted the circadian rhythms in sleep and locomotor activity but had smaller effects on body temperature that did not correlate significantly with vSPZ cell loss. By contrast, lesions of the dSPZ disrupted circadian rhythms in body temperature but had less of an effect on locomotor activity and virtually no effect on sleep. PVH lesions did not affect circadian rhythms of sleep, body temperature, or activity; however, the loss of neurons in the PVH significantly attenuated LPS-induced fever. The dSPZ lesions did not affect fever responses. These results suggest that the SPZ is a complex region consisting of neuronal subsystems that may differentially regulate circadian rhythms of different physiological responses. Conversely, the PVH appears to be an autonomic and endocrine effector site but does not play a major role in organizing circadian rhythms of sleep, activity, or body temperature.

Technical considerations

One potential problem was the anatomical proximity of the PVH to the dSPZ, raising the question of whether lesions of the dSPZ would also damage the PVH. Because the fibrous capsule of the PVH acts as a diffusion barrier to ibotenic acid, we were able to make cell-specific lesions in the dSPZ without damaging the PVH. We were also concerned that the close proximity of the vSPZ to the SCN might make it difficult to damage the vSPZ without affecting the SCN, lesions of which would disrupt all circadian rhythms. On the basis of histology of Nissl-, Fos-, AVP-, and VIP-stained sections through the SCN region, we found that SCN neurons were resistant to ibotenic acid [see also Peterson and Moore (1980)]. Moreover, after vSPZ lesions, body temperature retained a significant circadian rhythm, whereas sleep did not, which would not be expected if the effects were caused by SCN damage.

To define the border of the SPZ, we had to rely on the SCN terminal field, particularly the VIP-ir fiber zone. In our quantitative studies, we counted Nissl-stained neurons within the fields determined by these fibers. We recognize that other SCN outputs contain different neurotransmitters, but in our preliminary studies the course of the VIP-ir terminal field closely approximated the SCN output as judged in anterograde labeling from the SCN using biotinylated dextran (S. E. Gaus and C. B. Saper, unpublished observations).

The role of the subparaventricular zone in circadian regulation

The SPZ has traditionally been identified by tracing the efferent terminal field from the SCN, particularly its ventrolateral component (Watts and Swanson, 1987; Watts et al., 1987; Watts, 1991; Vrang et al., 1995). However, anatomical studies suggest dorsal and ventral regions within the SPZ that receive somewhat different inputs. For example, the vSPZ receives direct retinal afferents (Johnson et al., 1988; Mikkelsen, 1990), which may be important in reconstituting circadian cycles in a light/dark environment, even after SCN lesions. The dSPZ, by contrast, receives a substantial input from the dorsomedial part of the ventromedial hypothalamic nucleus (VMH) (Elmquist et al., 1998), which may be important in synchronizing circadian regulation with food availability (Challet et al., 1997; Choi et al., 1998). Our physiological observations support the separation of the SPZ into ventral and dorsal regions that differentially regulate circadian rhythms of sleep and body temperature.

The vSPZ lesions profoundly diminished the circadian rhythm of sleep and locomotor activity. Although these same lesions caused a statistically significant reduction in the circadian rhythm of body temperature, this function retained a significant degree of rhythmicity. More importantly, the loss of cells in the vSPZ correlated closely with the loss of sleep circadian rhythm but did not reach statistical significance for correlating with the loss of body temperature rhythm. These findings suggest that the changes in circadian rhythm of body temperature with the vSPZ lesions may have been caused by injury outside the vSPZ counting area, perhaps in the rostral edge of the dSPZ, which was included in some cases. Lesions of the dSPZ, by contrast, disrupted circadian control of body temperature (as judged by cosinor analysis or comparing day/night mean temperatures) to a significantly greater degree than did the vSPZ lesions ($p < 0.05$) but had no discernable effect on circadian rhythm of sleep or locomotor activity.

The differential role of the two SPZ regions in circadian control of sleep versus body temperature may be related to their connections. One prominent target of the SPZ is the preoptic area (Watts, 1991). Although relatively small in size, the preoptic area contains complex populations of cells that control body temperature, sleep, and reproduction (for review, see Satinoff, 1978; McGinty and Szymusiak, 1990; Argiolas, 1999). The medial pre-optic area, including the recently identified VMPO, plays an important role in

thermoregulation (Satinoff et al., 1982; Elmquist et al., 1996, Lu et al., 2000), whereas the ventrolateral preoptic nucleus (VLPO) plays a key role in the regulation of sleep (Sherin et al., 1996, 1998; Szymusiak et al., 1998; Lu et al., 2000). It will be important to determine whether projection from the dSPZ and vSPZ to the VMPO and VLPO may relay critical information for the differential circadian regulation of body temperature versus sleep.

The SPZ also projects to the DMH (Elmquist et al., 1998), which projects to many of the same preoptic targets as the SPZ. Previous studies have implicated the DMH in the circadian regulation of feeding, drinking, and corticosterone secretion (Bernardis, 1973; Bellinger et al., 1976; Cipolla-Neto et al., 1988; Kalsbeek et al., 1996). Our preliminary studies suggest that DMH lesions also have profound effects on circadian rhythms of sleep, locomotor activity, and body temperature (Chou et al., 2000). Hence the SPZ may act primarily as a link, integrating circadian input from the SCN and retina with behavioral inputs, e.g., from the VMH, and projecting to the DMH and preoptic targets to organize circadian responses.

The role of the paraventricular nucleus in circadian regulation

Compared with the SPZ, the PVH receives relatively small amounts of SCN inputs, mainly to its parvicellular subdivisions. Neurons in the PVH that are innervated by the SCN are thought to control sympathetic preganglionic cells that regulate melatonin secretion (Klein et al., 1983; Larsen et al., 1998; Teclemariam-Mesbah et al., 1999). Similarly, direct SCN projections to the PVH may regulate secretions of corticotrophin-releasing factor (Vrang et al., 1995b). The patterns of secretion of these hormones could potentially affect circadian rhythms of body temperature or sleep. To control for the possible effects of even minor damage to the PVH in our study, we analyzed the effect of ibotenic acid lesions of the nucleus on sleep, activity, and body temperature. Our results were consistent with earlier studies using electrolytic lesions of the PVH that had reported no major effects on body temperature (Horn et al., 1994) or the circadian regulation of sleep (Piepenbrock et al., 1985).

Our observations are consistent with the PVH being a target, rather than a pacesetter, for the circadian control system. The SPZ may influence the PVH via its projections to the DMH, which in turn provides substantial PVH input (Watts et al., 1987; Elmquist et al., 1998).

Regulation of ultradian rhythms

The emergence of ultradian rhythms after lesions in the SCN and SPZ suggests that ultradian rhythms are generated by different mechanisms and suppressed by circadian rhythms generated by the SCN and SPZ. Large electrolytic lesions in the SCN region and the adjacent retrochiasmatic area or lesions in the retrochiasmatic area–arcuate nucleus eliminate ultradian rhythms of sleep (Wollnik and Turek, 1989; Gerkema et al., 1990), suggesting that the retrochiasmatic area may play a role in ultradian oscillation. Although ultradian rhythms are relatively weak in the presence of circadian control, they may still be recognized, especially during the night (wake period), as shown by the ultradian rhythm in delta power (Fig. 5*A*).

The paraventricular nucleus and the febrile response

Several lines of circumstantial evidence suggest that the PVH plays an important role in the fever response. Large number of Fos-active cells are seen in the PVH during fever in rats produced either by intravenous or intraperitoneal LPS (Elmquist et al., 1996; Konsman et al., 1999) or by interleukin-1β (Rivest et al., 1992; Ericsson et al., 1994; Day and Akil, 1996). Parvicellular neurons in the dorsal PVH are Fos positive during fever and project directly to the sympathetic preganglionic column in the spinal cord (Zhang et al., 2000). This pathway may play an important role in fever response by stimulating brown adipose

tissue to produce heat by activating the uncoupling protein UCP1, causing the adrenal glands to secrete adrenaline, and constricting the tail artery to reduce cutaneous heat loss (for review, see Zhang et al., 2000). Electrolytic lesions of the PVH decrease fever responses without affecting responses to a cold or hot environment (Horn et al., 1994). Our studies using excitotoxic lesions further support the role of the PVH as a key site for regulating fever response but not circadian rhythm of body temperature.

Acknowledgments

This research was supported by National Institutes of Health Grants NS 33987 and MH55772. We thank Quan Hue Ha, Joseph F. Kelly, and Charlotte Lee for excellent technical help.

References

Argiolas A. Neuropeptides and sexual behaviour. Neurosci Biobehav Rev. 1999; 23:1127–1142. [PubMed: 10643821]

Bellinger LL, Bernardis LL, Mendel VE. Effect of ventromedial and dorsomedial hypothalamic lesions on circadian corticosterone rhythms. Neuroendocrinology. 1976; 22:216–225. [PubMed: 1028952]

Bernardis LL. Disruption of diurnal feeding and weight gain cycles in weanling rats by ventromedial and dorsomedial hypothalamic lesions. Physiol Behav. 1973; 10:855– 861. [PubMed: 4715812]

Challet E, Pevet P, Lakhdar-Ghazal N, Malan A. Ventromedial nuclei of the hypothalamus are involved in the phase advance of temperature and activity rhythms in food-restricted rats fed during daytime. Brain Res Bull. 1997; 43:209–218. [PubMed: 9222534]

Choi S, Wong LS, Yamat C, Dallman MF. Hypothalamic ventromedial nuclei amplify circadian rhythms: do they contain a food-entrained endogenous oscillator? J Neurosci. 1998; 18:3843–3852. [PubMed: 9570813]

Chou TC, Scammell TS, Lu JL, Shromani PJ, Saper CB. Excitotoxic lesions of the dorsomedial hypothalamic nucleus markedly attenuate circadian rhythms of sleep and body temperature. Soc Neurosci Abstr. 2000; 26:469.9.

Cipolla-Neto J, Afeche SC, Menna-Barreto L, Marques N, Benedito-Silva AA, Fortunato G, Recine EG, Schott C. Lack of similarity between the effect of lesions of the suprachiasmatic nucleus and sub-paraventricular hypothalamic zone on behavioral circadian rhythms. Braz J Med Biol Res. 1988; 21:653– 654. [PubMed: 3228652]

Day HE, Akil H. Differential pattern of c-fos mRNA in rat brain following central and systemic administration of interleukin-1-beta: implications for mechanism of action. Neuroendocrinology. 1996; 63:207–218. [PubMed: 8677009]

Dunlap JC. Common threads in eukaryotic circadian systems. Curr Opin Genet Dev. 1998; 8:400–406. [PubMed: 9729714]

Eastman CI, Mistlberger RE, Rechtschaffen AA. Suprachiasmatic nucleus lesions eliminate circadian temperature and sleep rhythms in the rat. Physiol Behav. 1984; 32:357–368. [PubMed: 6463124]

Elmquist JK, Scammell TE, Jacobson CD, Saper CB. Distribution of Fos-like immunoreactivity in the rat brain following intravenous lipopolysaccharide administration. J Comp Neurol. 1996; 371:85–103. [PubMed: 8835720]

Elmquist JK, Ahima RS, Elias C, Flier J, Saper CB. Leptin activates distinct projections from the dorsomedial and ventromedial hypothalamic nuclei. Proc Natl Acad Sci USA. 1998; 95:741–746. [PubMed: 9435263]

Ericsson A, Kovacs KJ, Sawchenko PE. A functional anatomical analysis of central pathways subserving the effects of interleukin-1 on stress-related neuroendocrine neurons. J Neurosci. 1994; 14:897–913. [PubMed: 8301368]

Gerkema MP, Groos GA, Daan S. Differential elimination of circadian and ultradian rhythmicity by hypothalamic lesions in the common vole, *Microtus arvalis*. J Biol Rhythms. 1990; 5:81–95. [PubMed: 2133128]

Harrington, ME.; Rusak, B.; Mistlberger, RE. Anatomy and physiology of the mammalian circadian system. In: Kryger, MH.; Roth, T.; Dement, WC., editors. Principles and practice of sleep and medicine. Philadelphia: W. B. Saunders; 1994. p. 286-300.

Horn T, Wilkinson MF, Landgraf R, Pittman QJ. Reduced febrile response to pyrogens after lesions of the hypothalamic paraventricular nucleus. Am J Physiol. 1994; 36:R323–R328. [PubMed: 8048639]

Ibuka N, Kawamura H. Loss of circadian rhythm of sleep-wakefulness cycle in the rats by suprachiasmatic nucleus lesions. Brain Res. 1975; 96:76– 81. [PubMed: 1175007]

Johnson RF, Morin LP, Moore RY. Retinohypothalamic projections in the hamster and rat demonstrated using cholera toxin. Brain Res. 1988; 462:301–312. [PubMed: 3191391]

Kalsbeek A, Drijfhout WJ, Westerink BH, van Heerikhuize JJ, van der Woude TP, van der Vliet J, Buijs RM. GABA receptors in the region of the dorsomedial hypothalamus of rats were implicated in the control of melatonin and corticosterone. Neuroendocrinology. 1996; 63:69–78. [PubMed: 8839357]

Klein DC, Smoot R, Weller JL, Higa S, Markey SP, Greed GJ, Jacobowitz DM. Lesions of the paraventricular nucleus area of the hypothalamus disrupt the suprachiasmatic leads to spinal cord circuit in the melatonin rhythm generating system. Brain Res Bull. 1983; 10:647– 652. [PubMed: 6307491]

Konsman JP, Kelley K, Dantzer R. Temporal and spatial relationships between lipopolysaccharide-induced expression of Fos, interleukin-1beta and inducible nitric oxide synthase in rat brain. Neuroscience. 1999; 89:535–548. [PubMed: 10077334]

Larsen PJ, Enquist LW, Card JP. Characterization of the multi-synaptic neuronal control of the rat pineal gland using viral transneuronal tracing. Eur J Neurosci. 1998; 10:128–145. [PubMed: 9753120]

Lu J, Greco MA, Shiromani P, Saper CB. The effects of lesions of ventrolateral preoptic nucleus on NREM and REM sleep. J Neurosci. 2000; 20:3830–3842. [PubMed: 10804223]

McGinty D, Szymusiak R. Keeping cool: a hypothesis about the mechanisms and functions of slow-wave sleep. Trends Neurosci. 1990; 13:480– 487. [PubMed: 1703678]

Mikkelsen JD. Projections from the lateral geniculate nucleus to the hypothalamus of the mongolian gerbil (Meriones unguiculatus): an anterograde and retrograde tracing study. J Comp Neurol. 1990; 299:493–508. [PubMed: 1700802]

Mouret J, Coindet J, Debilly G, Chouvet G. Suprachiasmatic nuclei lesions in the rat: alterations in sleep circadian rhythms. Electroencephalogr Clin Neurophysiol. 1978; 45:402– 408. [PubMed: 79478]

Paxinos, G.; Watson, C. The rat brain in stereotaxic coordinates. San Diego: Academic; 1986.

Peterson GM, Moore RY. Selective effects of kainic acid on diencephalic neurons. Brain Res. 1980; 24:165–182. [PubMed: 7427732]

Piepenbrock N, Valatx JL, Malquarti V, Jouvet M. Effects of hypothalamic paraventricular lesions on sleep in rats. Neurosci Lett. 1985; 62:151–156. [PubMed: 3911117]

Rivest S, Torres G, Rivier C. Differential effects of central and peripheral injection of interleukin-1 beta on brain c-fos expression and neuroendocrine functions. Brain Res. 1992; 587:13–23. [PubMed: 1326374]

Saper, CB. Central autonomic system. In: Paxinos, G., editor. The rat nervous system. San Diego: Academic; 1995. p. 107-135.

Satinoff E. Neural organization and evolution of thermal regulation in mammals. Science. 1978; 201:16–22. [PubMed: 351802]

Satinoff E, Liran J, Clapman R. Aberrations of circadian body temperature rhythms in rats with medial preoptic lesions. Am J Physiol. 1982; 201:R352–R357. [PubMed: 7065231]

Sherin JE, Shiromani PJ, McCarley RW, Saper CB. Activation of ventrolateral preoptic neurons during sleep. Science. 1996; 271:216–219. [PubMed: 8539624]

Sherin JE, Elmquist JK, Tooealba F, Saper CB. Innervation of histaminergic tuberomammillary neurons by GABAergic and galanergic neurons in the ventrolateral preoptic nucleus of the rat. J Neurosci. 1998; 18:4705– 4721. [PubMed: 9614245]

Szymusiak R, Alam N, Steininger TC, McGinty D. Sleep-waking discharge patterns of ventrolateral preoptic/anterior hypothalamic neurons in rats. Brain Res. 1998; 803:178–188. [PubMed: 9729371]

Teclemariam-Mesbah R, Ter Horst GJ, Fostema F, Wotel J, Buijs RM. Anatomical demonstration of the suprachiasmatic nucleus-pineal gland. J Comp Neurol. 1999; 406:171–182. [PubMed: 10096604]

Vrang N, Larsen PJ, Moller M, Mikkelsen JD. Topographical organization of the rat suprachiasmatic-paraventricular projection. J Comp Neurol. 1995a; 353:585– 603. [PubMed: 7759617]

Vrang N, Larsen PJ, Mikkelsen JD. Direct projection from the suprachiasmatic nucleus to hypophysiotrophic corticotropin-releasing factor immunoreactive cells in the paraventricular nucleus of the hypothalamus demonstrated by means of *Phaseolus vulgaris*-leucoagglutinin tract tracing. Brain Res. 1995b; 684:61– 69. [PubMed: 7583205]

Watts, AG. The efferent projections of the suprachiasmatic nucleus: anatomical insights into the control of circadian rhythms. In: Klein, DC.; Moore, RY.; Reppert, SM., editors. Suprachiasmatic nucleus: the mind's clock. New York: Oxford UP; 1991. p. 77-106.

Watts AG, Swanson LW. Efferent projections of the suprachiasmatic nucleus: II. Studies using retrograde transport of fluorescent dyes and simultaneous peptide immunohistochemistry in the rat. J Comp Neurol. 1987; 258:230–252. [PubMed: 2438309]

Watts AG, Swanson LW, Sanchez-Watts G. Efferent projections of the suprachiasmatic nucleus: I. Studies using anterograde transport of *Phaselous vulgaris* leucoagglutinin in rat. J Comp Neurol. 1987; 258:204–229. [PubMed: 3294923]

Wollnik F, Turek FW. SCN lesions abolish ultradian and circadian components of activity rhythms in LEW/Ztm rats. Am J Physiol. 1989; 265:R1027–R1039. [PubMed: 2785771]

Zhang YH, Lu JL, Elmquist JK, Saper CB. Lipopolysaccharide activates specific populations of hypothalamic and brainstem neurons that project to the spinal cord. J Neurosci. 2000; 20:6578–6586. [PubMed: 10964963]

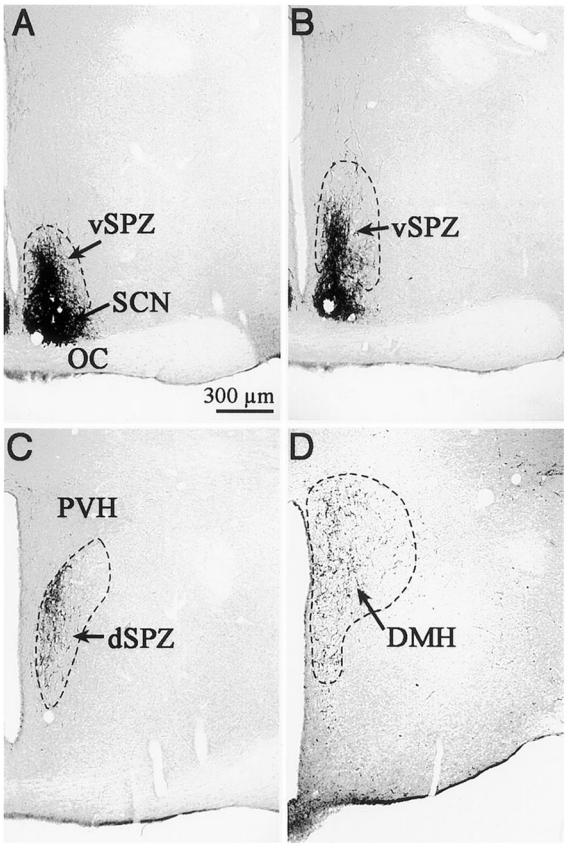

Figure 1.

Photomicrographs showing VIP-ir axons and terminals that define the subparaventricular zone (*SPZ*) from rostral to caudal levels. *A*, *B*, The ventral SPZ demonstrated by a column of VIP-ir axons leaving the dorsal margin of the suprachiasmatic nucleus (*SCN*). *C*, The dorsal SPZ, ventral to the paraventricular nucleus (*PVH*). Notice the VIP-ir terminals in the medial PVH. *D*, The continuation of VIP-ir terminals from the SCN into the rostral DMH.

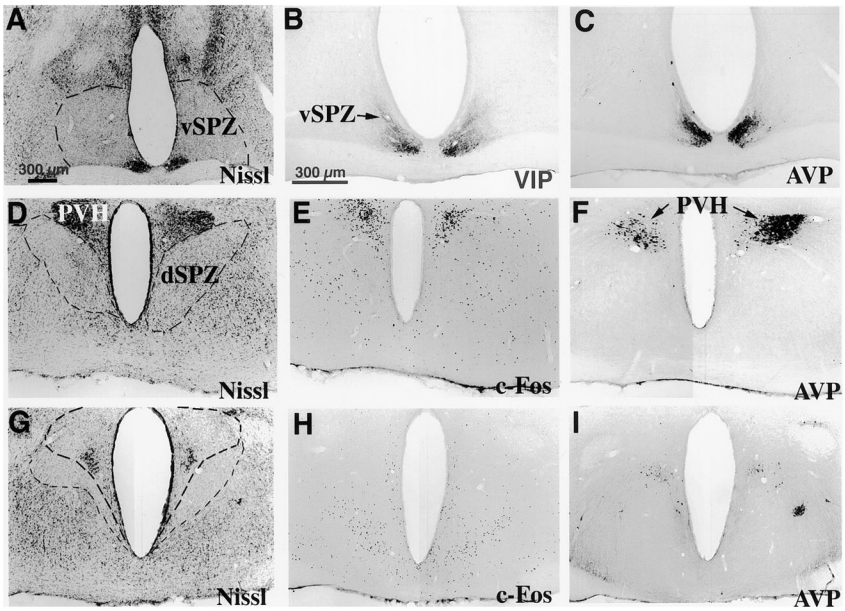

Figure 2.

Photomicrographs showing lesions (outlined by *light dashed line*) in the ventral SPZ (*A–C*, *vSPZ*), dorsal SPZ (*D–F*, *dSPZ*), and PVH (*G–I*). Lesions of the vSPZ typically spared the SCN as confirmed by immunostaining for VIP and AVP (*A–C*). Lesions of the dSPZ (*D*) did not affect the PVH, as shown by immunostaining for Fos (*E*, induced by LPS) and AVP (*F*). Lesions of the PVH (*G*, PVH border outlined in *heavy dashed line*) were verified by loss of Fos-ir neurons after LPS injection and by loss of AVP-ir neurons (*H, I*).

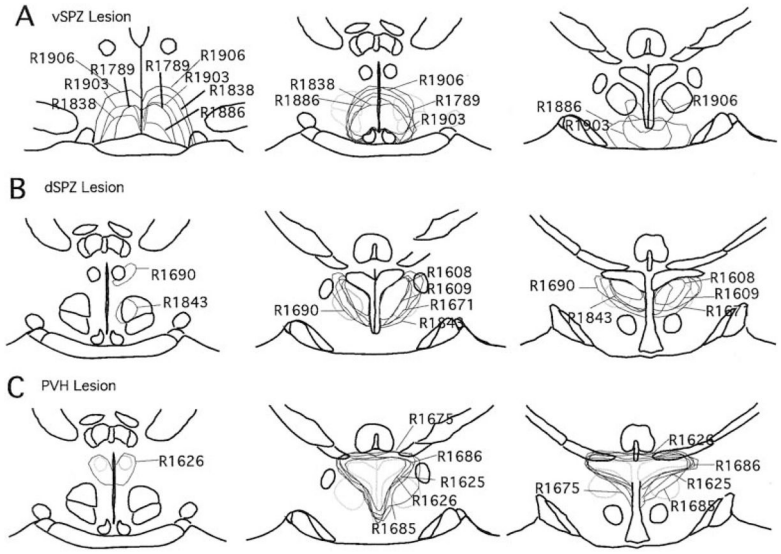

Figure 3.
A series of camera lucida drawings illustrating lesion areas in the vSPZ (*A*), dSPZ (*B*), and PVH (*C*).

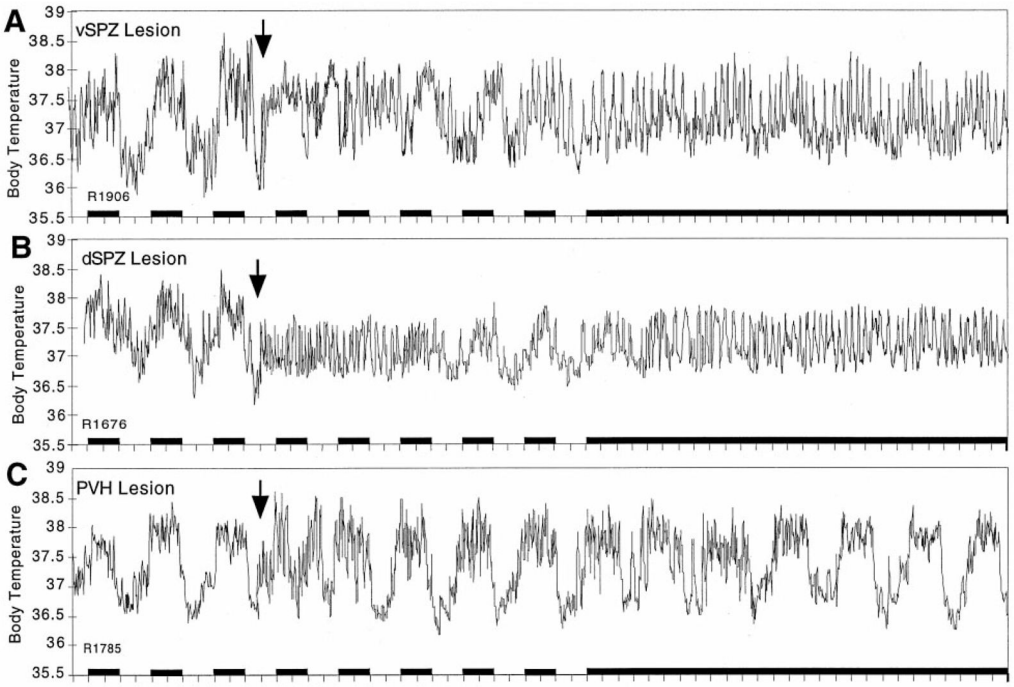

Figure 4.

Plots showing long-term effects of representative lesions of the vSPZ (*A*), dSPZ (*B*), and PVH (*C*) on body temperature. After the vSPZ lesion (*A*), body temperature showed a decreased circadian amplitude but still retained a circadian rhythm even under constant darkness (subjective day vs night mean value different at $p < 0.05$), which could be recognized visually in the long-term recording of body temperature. The dSPZ lesion (*B*) initially disrupted body temperature rhythm, which slowly recovered and showed a low amplitude during light/dark cycle conditions. However, in constant darkness the circadian rhythm of body temperature was lost almost completely. In contrast, the rat with PVH lesions (*C*) showed a normal circadian rhythm in body temperature under both light/dark and constant darkness conditions. The *arrow* indicates the time of placing the lesions. *Black bars* represent the periods of darkness.

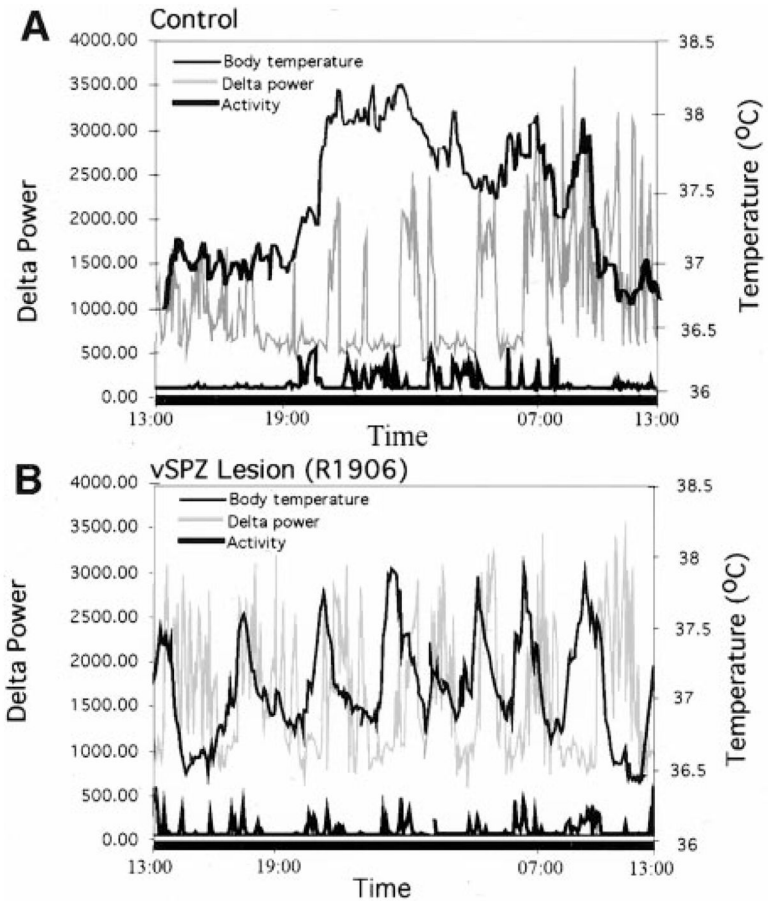

Figure 5.

Combined graphs showing EEG delta power (*gray line*), body temperature (*light black line*), and locomotor activity (*heavy black line*) under constant darkness in a representative control animal (*A*) and in an animal with a vSPZ lesion (*B*). The *left y*-axis demarcates delta power, the *right y*-axis shows body temperature, and the *x*-axis is time = 24 hr. Locomotor activity is in arbitrary units. The control rat (*A*) showed robust circadian rhythms of EEG delta power, body temperature, and activity. Sleep was increased predominantly during the subjective day, whereas body temperature and activity were increased during the subjective night. After a vSPZ lesion (*B*), there was a loss of circadian variation in delta power and activity.

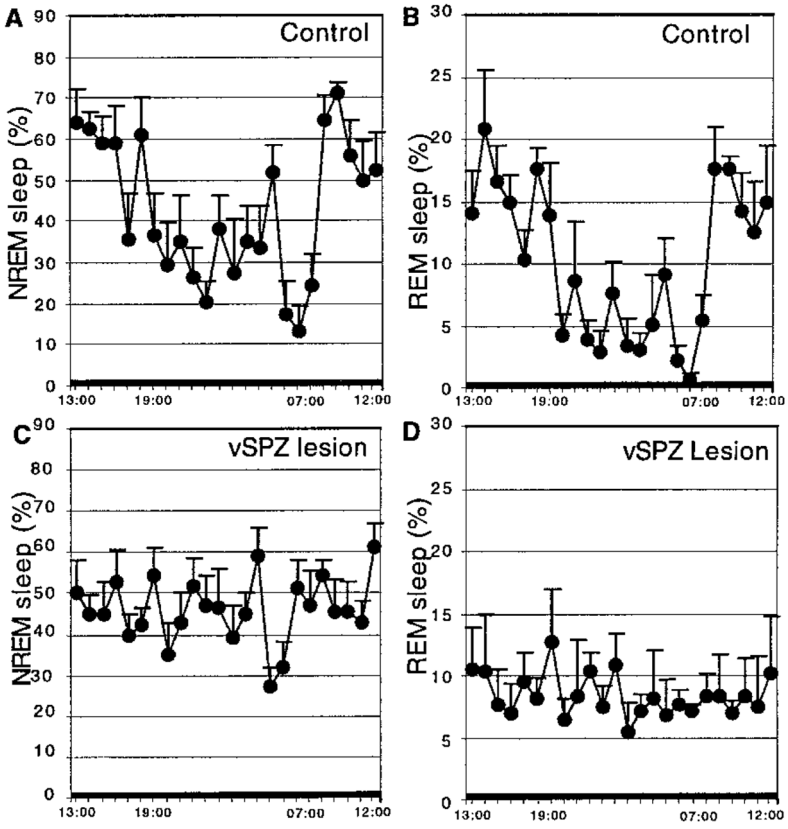

Figure 6.

Percentage rapid eye movement (*REM*) sleep per hour and non-REM (*NREM*) sleep per hour across 24 hr (constant darkness) in controls (*A*, *B*) and vSPZ lesioned rats (*C*, *D*). There was loss of circadian variation in both REM and NREM sleep after lesions in the vSPZ, whereas both REM and NREM sleep showed a robust circadian rhythm in the control group.

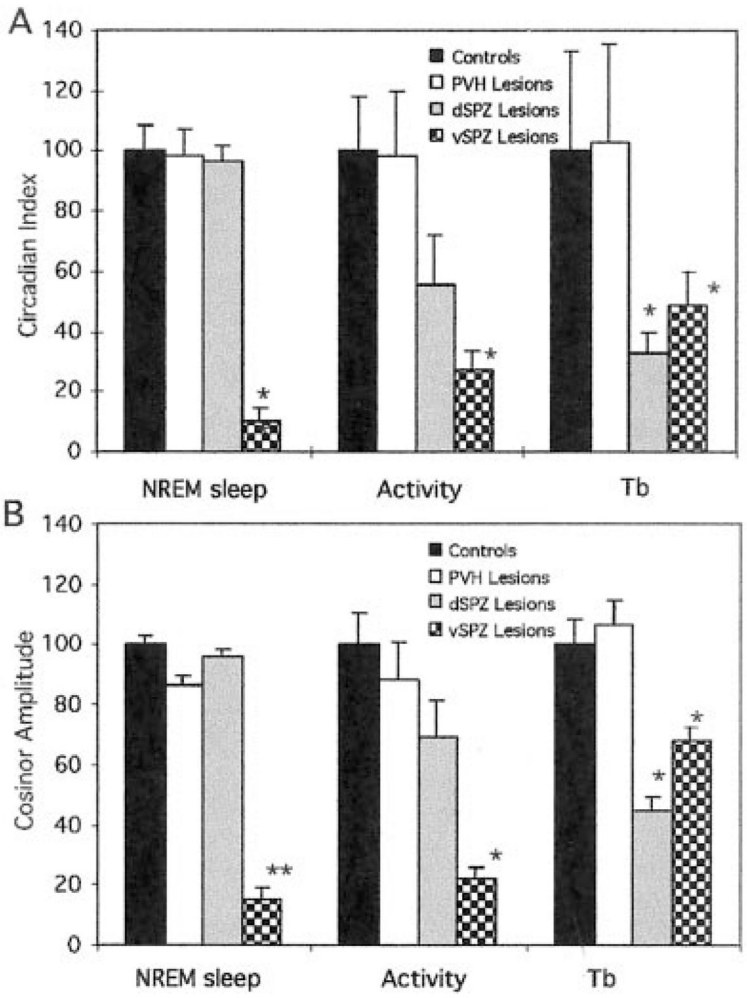

Figure 7.

The effects of lesions in the dSPZ, vSPZ, and PVH on circadian index (*A*) and cosinor amplitude (*B*) of NREM sleep, body temperature (*Tb*), and activity under constant darkness. The circadian index and cosinor amplitude were normalized to the mean circadian amplitude of the control animals (100). The dSPZ lesions significantly reduced the circadian index of body temperature but did not significantly affect circadian index or cosinor amplitude of NREM sleep or activity. The vSPZ lesions dramatically reduced circadian index and cosinor amplitude for sleep and activity and had somewhat less intense, although still significant, effects on body temperature. $*p < 0.05$; $**p < 0.01$.

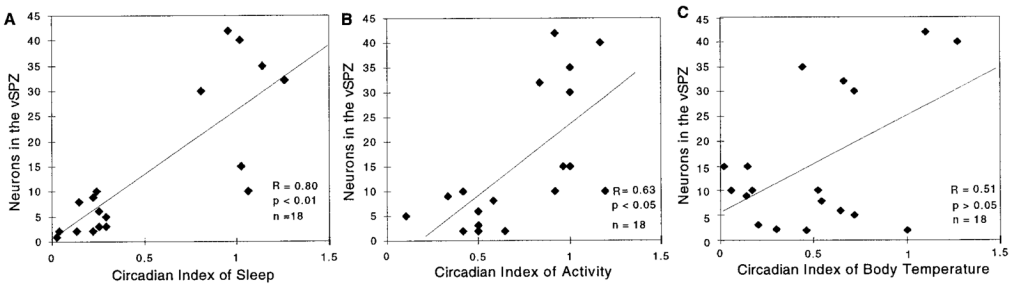

Figure 8.

Correlation of the number of surviving neurons in the vSPZ with the circadian index of body temperature, sleep, and locomotor activity. For sleep and activity, there was a significant ($p < 0.05$) linear correlation of circadian index with the number of surviving neurons in the vSPZ, whereas the circadian index of body temperature did not show a significant correlation ($p > 0.05$), suggesting that alterations of body temperature rhythm may have been caused by the lesions including tissue beyond the vSPZ counting box.

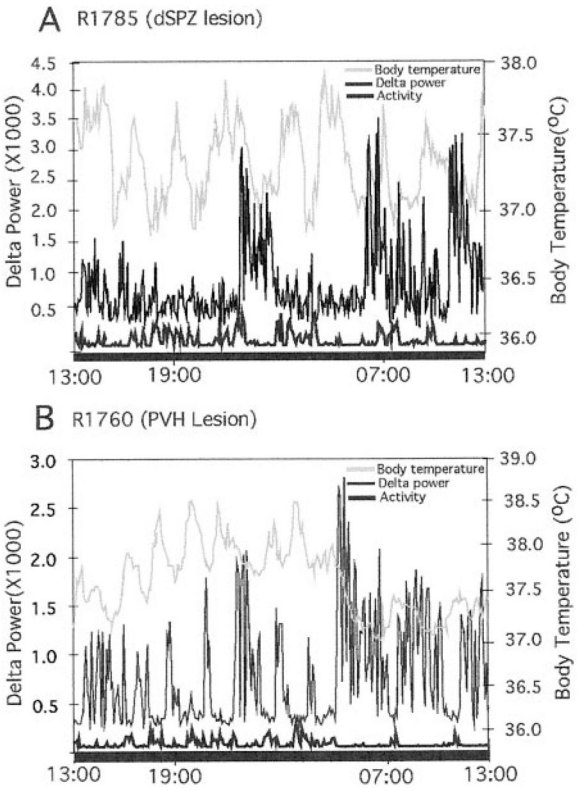

Figure 9.

Combined graphs showing the effects on EEG delta power (*light black line*), locomotor activity (*heavy black line*), and body temperature (*gray line*) of lesions in the dSPZ (*A*) and the PVH (*B*). The *left y*-axis demarcates delta power, the *right y*-axis shows body temperature, and the *x*-axis is time = 24 hr. Locomotor activity is in arbitrary units. After a dSPZ lesion (*A*), there was loss of circadian rhythm in body temperature, but delta power and activity from the same animal showed a clear circadian rhythm. In *B* (PVH lesion), body temperature, EEG delta power, and locomotor activity all showed robust circadian rhythms.

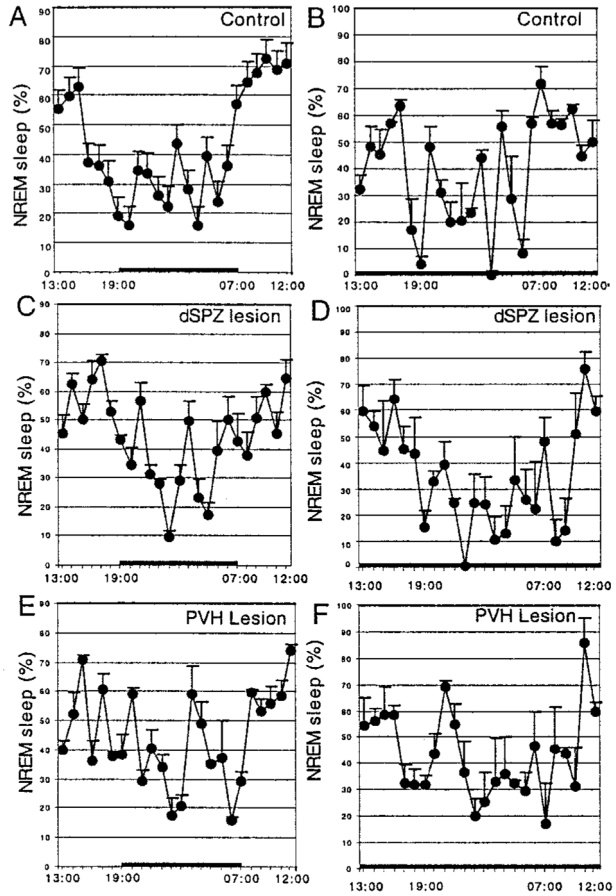

Figure 10.

Circadian rhythms of the percentage NREM sleep during a 12 hr light/dark cycle (*A*, *C*, *E*) and under constant darkness (*B*, *D*, *F*), in controls (*A*, *B*), and after lesions of the dSPZ (*C*, *D*) or PVH (*E*, *F*). Neither lesion significantly affected circadian rhythms of NREM sleep compared with controls.

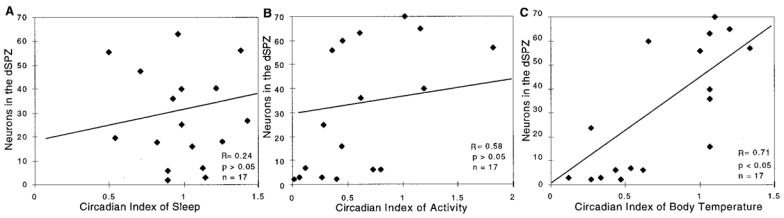

Figure 11.

Correlation of the numbers of surviving neurons in the dSPZ plotted against the circadian index of sleep (*A*), locomotor activity (*B*), and body temperature (*C*). The circadian index of body temperature but not sleep or activity showed a strong correlation with the numbers of surviving neurons (per side) in the dSPZ.

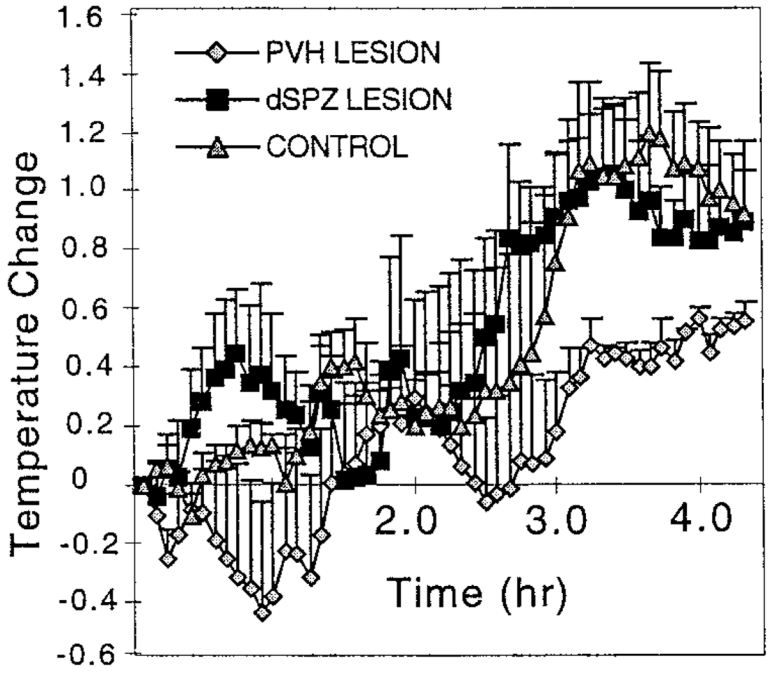

Figure 12.

Fever responses in rats with lesions in the PVH (*gray diamonds*), dSPZ (*black squares*), or controls (*gray triangles*) after intravenous LPS injection. The PVH lesion significantly attenuated fever (66.6%; $p < 0.01$) compared with the controls. In contrast, the rats with dSPZ lesions showed fever responses that did not differ significantly from the controls ($p > 0.05$). The injection time is at zero on the *x*-axis.

Table 1

Fos-immunoreactive neurons in the brain after intravenous

Brain area	No lesion	dSPZ lesion	PVH lesion
VMPO	44.6 ± 15.0	49.7 ± 12.0	44.6 ± 6.4
PVH	56.2 ± 8.2	53.1 ± 7.1	9.5 ± 0.9
NTS	41.8 ± 20.3	49.3 ± 6.5	49.4 ± 12.6

Numbers of Fos-immunoreactive neurons per section, on one side of the brain, in the VMPO, PVH, and NTS, after 5 μg/kg of intravenous lipopolysaccharide, in rats with no lesions or in animals with lesions of the dSPZ or PVH.